

Case Inst Tech
SEMI-ANNUAL REPORT
NASA RESEARCH GRANT NGR-36-003-100

Introduction

During the period covered by this report several aspects of the research have been carried forth, (1) initial measurements and interpretation of the homogeneity of Thailand tektites have been accomplished; (2) measurements on the self-diffusion of Si^{4+} , Sr^{2+} , and K^{+} have been nearly completed in the system $\text{K}_2\text{O} - \text{SrO} - \text{SiO}_2$; (3) a paper relating to multicomponent diffusion in silicates has been revised and accepted for publication; (4) a brief paper has been prepared for presentation at the Conference on Mass Transport sponsored by N.B.S. and A.R.P.A. A copy of the paper mentioned in item #3 is attached, and a paper will shortly be put in form for publication conveying item #4. Thus, this report will primarily discuss items #1 and #2. These will be treated separately.

GPO PRICE \$ _____

CFSTI PRICE(S) \$ _____

Hard copy (HC) 3.00

Microfiche (MF) _____

FACILITY FORM 802

N67-40337

(ACCESSION NUMBER)

33

(PAGES)

CR-89773

(NASA CR OR TMX OR AD NUMBER)

(THRU) _____

1

(CODE)

18

(CATEGORY)

1. Homogeneity of Tektites

Sample Preparation

(a) Glass Melts

Using oxides and carbonates several batches were calculated to make glasses in the vicinity of the following composition: (in weight per cent)

SiO_2	72
Al_2O_3	13
Fe_3O_4	5.8
MgO	2.7
CaO	1.9
Na_2O	1.5
K_2O	2.3
TiO_2	0.7
MnO	0.1

First melting attempts were made in platinum crucibles at 1500°C. While glasses were obtained, they were too viscous to pour and adhered so strongly to the crucible that alkali carbonate fusions were required to remove glass from crucible. An alternative technique of melting in silica crucibles proved satisfactory.

Although pouring and stirring were still impossible due to the high viscosity of the melt, the crucibles are relatively inexpensive and expendable. Melts made at 1500°C for 30 hours proved to appear homogeneous (the black color makes homogeneity observation much less critical

than it is for transparent glass).

The main limitation of this melting practice was the fairly high seediness (bubbles about 0.5 mm in diameter) of the glass. This is, no doubt, related to the extremely high viscosity of the melt. However, perhaps for the same reason, solution of the silica refractory was undetectable.

The glasses are sufficiently free from bubbles to permit electron probe analysis, but it was deemed inadvisable to perform diffusion measurements using these glasses.

This glass plus a Thailand Tektite (#2172) and a synthetic glass tektite^{*} were sectioned and polished for homogeneity study with the electron probe. The tektite had roughly speaking cylindrical symmetry about its long axis and, of course, crucible melts also had cylindrical symmetry. A numbering convention was thus adopted which has odd numbers referring to sections normal to "cylindrical" axis and even numbers reserved for sections containing cylindrical axis.

The samples were coated with an approximately 200A^o thick coating of carbon and their homogeneity was analyzed with a Mac Electron Microprobe.

*supplied by Roy S. Clarke, Smithsonian Institute

Electron Microprobe Procedures

Conditions of operation for the electron microprobe for the major elements studied are shown in Table I.

Three different procedures were used. A general observation of the homogeneity was obtained by taking photographs of the X-ray fluorescence of the various elements when the tektite samples were scanned with the electron beam to produce a raster.

A second technique was to use a "spot" and "step scan" across the sample in steps of 10μ until (usually) 100 readings were taken. The coefficient of variation was compared with the variation from repeated countings at a single spot. Usually only 10 or 20 individual readings were taken.

The final procedure was designed to look at longer range fluctuations, and here a raster $10\mu \times 10\mu$ was scanned, and the region was counted five separate times. Then the raster was moved about 1 mm and the process repeated. This continued until the entire width of the sample (~ 1 cm) was traversed. A similar procedure was carried out by taking repeated sets of readings with the raster in the same position.

Programs were written for obtaining the means and the standard deviations either of individual values or of averages of sets of five values.

TABLE I

PROBE CONDITIONS FOR VARIOUS ELEMENTS

For Fe

Flow proportional counter with P-10

LiF crystal

Radiation: $K\alpha = 1.932 \text{ \AA}$

25 KV Gun Voltage

0.03 ma specimen current

Spectrometer to air

No slit

Background on pure Co specimen

Suggested peak/background for Fe $\approx 350/1$

For Si

Flow proportional counter with P-10

PET crystal

Radiation: $K\alpha = 7.111 \text{ \AA}$

20 KV Gun Voltage

0.03 ma specimen current

Spectrometer in Vacuum

No slit

Background on pure Al specimen

Suggested peak/background for Si $\approx 2600/1$

For Al

Flow proportional counter, P-10 gas

KAP crystal

Radiation: $K\alpha = 8.320 \text{ \AA}$

20 KV Gun Voltage

0.03 ma specimen current

Spectrometer to vacuum

No slit

Background on pure Si specimen

Suggested peak/background for Al $\approx 250/1$

Results

An indication of the compositional variation for a variety of elements is shown in the photographs of the X-ray fluorescence at appropriate wave lengths when the sample was scanned (Plate 1).

The main body of quantitative results on tektite and synthetic glass homogeneity are shown in Table II, Table III, Fig. 1 (a thru g) and Fig. 2 (a thru e).

Table II compares the coefficient of variation for various samples when step-scanned with the coefficient of variation for repeated counts in the same position.

Table III compares the coefficient of variation of average of sets of five counts from a $10\mu \times 10\mu$ raster which is moved, to its calculated coefficient of variation when stationary.

TABLE II

COMPARISON OF COEFFICIENT OF VARIATION, (σ / \bar{x}) FOR
LOCAL AND STEP-SCANNED ANALYSIS OF TEKTITE

	<u>Local</u>	<u>Stepped</u>
Aluminum #1	.022	.025
#2	.019	.043
Silicon #1	.017	.039
#2	.023	.044
Iron #1	.016	.032
#2	.041	.045
Aluminum #8 *	.021	.020

*Synthetic tektite melted at Case-WRU

TABLE III

COMPARISON OF COEFFICIENT OF VARIATION $\left\{ \frac{\sigma}{\bar{X}_5} \right\}$ (FOR
AVERAGE OF SETS OF FIVE) IN LOCAL POSITION WITH
COEFFICIENT WHEN RASTER IS MOVED.

<u>Specimen</u>	<u>Local</u>	<u>Moved</u>
Aluminum #1	0.010	0.030
#2	0.009	0.022
Silicon #1	0.015	0.038
#2	0.016	0.070
Iron #1	0.017	0.037
#2	0.013	0.023

Figure 1 shows the compositional variation with position within a 1 mm distance for several elements on two sections of a Thailand Tektite. The average values and a normalized 3σ limit is shown on each of the plots. The normalized value of σ was obtained by taking the coefficient of variation in the local position (Table II) and multiplying it by the mean value of counts for the step-scanned results.

Fig. 2 shows compositional variation with position on a larger scale.

Discussion

Plate 1 shows that there is no gross compositional heterogeneity of Al, Si, Fe, K, or Ca within the Thailand Tektite that was examined. The local mottled appearance of the photographs is necessary to permit any evaluation for long range non-uniformity.

The information in Tables II and III reveals that there are concentration fluctuations with positions both within a single millimeter traverse (Table II) and over a much longer distance scale (Table III). This is revealed by the fact that the coefficient of variation is invariably larger for the counts when the sample is moved than for series of counts taken in the same position. When the steps are at small intervals (100 steps within a mm) Table II

shows that the average coefficient of variation is 1.8 times greater for the scanned sample than for a local position. When steps are longer (about 1 mm each), Table III shows that the coefficient of variation is about $2 \frac{2}{3}$ times greater for the stepped raster than for the stationary raster.

If the counts are assumed to come from a normal population, then the normalized variances, $V = \left(\frac{\sigma}{\bar{x}} \right)^2$, should be additive. In other words, we could say:

$$V_{\text{scanned}} = V_{\text{local}} + V_{\text{position}} \quad (1)$$

where V_{position} is the variance due solely to concentration fluctuations with position.

Using Eq. #1 the indications from Table II are that the coefficient of variation, $(V_{\text{position}})^{1/2}$, due to concentration fluctuations with position within a 1 mm region might be as high as 0.04 for the elements studied. This is slightly higher than reported by Walter* for SiO_2 and about the same as he found for Al_2O_3 .

A glance at the figures shows qualitative support for this premise. Fig. 2b shows what appears to be a fluctuation of Al_2O_3 content with an intensity of about 10% of the average concentration and a scale of about 250-300 μ . Figures 1c and 1d can be interpreted as showing a fluctuation of similar magnitude. Since the iron counts always remain within the 3σ limits, it is less certain whether the variations shown on Fig. 2e and 2f are due to fluctuations with position or just unrelated noise.

* L. Walter, 'Tektite Compositional Trends and Experimental Vapor Fractionation of Silicates' NASA Report X-641-67-221

The data in Table III and results in Fig. 2 are more convincing in demonstrating that concentration fluctuations with position do exist. It is not certain, however, whether this greater certainty is primarily due to the use of sets of five readings which tend to diminish the values of $\left\{ \frac{\sigma}{\bar{x}} \right\}_5$ compared with $\left\{ \frac{\sigma}{\bar{x}} \right\}_{\text{local}}$ or the fact that larger distance scales are involved. In either event, the data particularly in 2e and 2d suggest concentration fluctuations of $\pm (0.05 \times 72\%) \approx \pm 4\%$ with a scale of perhaps 0.5 cm.

The results (Table II and Fig. 1g) show that the aluminum variation with position in the synthetic tektite made at Case-WRU is slightly less than the natural samples.

While the data is not yet of sufficient precision to allow us to interpret the results rigorously in terms of a quantitative description of the homogeneity, it seems clear that the tektites are not perfectly homogeneous. On the other hand, the fluctuations in concentration do appear to be of rather modest intensity.

PLANS FOR FUTURE WORK

In order to draw conclusions regarding possible origins of tektites, four separate pieces of information are needed:

- i a proposed origin including minerals and their spatial distribution
- ii an estimate of deformation during origin
- iii a measure of concentration fluctuations in tektite
- iv an estimate of diffusion coefficients

For items i, and ii we need outside help. Item iii has been the subject of most of this report. To improve on this we need a better experimental design, and it is expected that with the help of our mathematics department, particularly Professor C. Bell, this will be achieved during the next six months.

For item iv we need to start with glass melts that are free from bubbles in order that convection due to bubble motion will not distort the results. At present we are planning longer time melting experiments in silica at 1500°C (up to 300 hours) or in graphite or refractory metals at higher temperatures.

Diffusion couples from glasses of different compositions in the range of tektite glasses will be given diffusion anneals at various times and temperatures.

2. SELF-DIFFUSION IN $K_2O-SrO-SiO_2$ SYSTEM

The following radioactive isotopes are obtained by the neutron irradiations of a $K_2O-SrO-SiO_2$ glass:

TABLE IV

	<u>Isotope</u>	<u>Half Life</u>	<u>Radiation emitted</u>
(1)	Si^{31}	2.6 h	1.47 meV β^- \sim 99.97% 1.26 meV γ \sim 0.03%
(2)	K^{42}	12.4 h	3.56 meV β^- \sim 82% 2.04 meV β^- \sim 18% 1.51 meV γ \sim 18%
(3)	Sr^{85m}	70 m	0.225 meV γ \sim 85%
(4)	Sr^{85}	64 d	0.513 meV γ \sim 100%
(5)	Sr^{87m}	2.8 h	0.39 meV γ 100%
(6)	Sr^{89}	51 d	1.46 meV β^- 100%

The table indicates suitability of K^{42} , Sr^{87m} and Sr^{85} for self-diffusion studies, particularly in case of Sr where a short-lived and a long-lived isotope emitting γ particles are produced. γ particles are easy to characterize and do not present any difficulties with regard to their counting.

The short half life of Si^{31} and the fact that the

dominant radiation from the decay is β particles cause considerable difficulties in the detection of Si^{31} . Thus, diffusion anneals can only be carried out for short periods and techniques for separation from the β particles of K^{42} and Sr^{89} have to be employed.

Diffusion Couple:

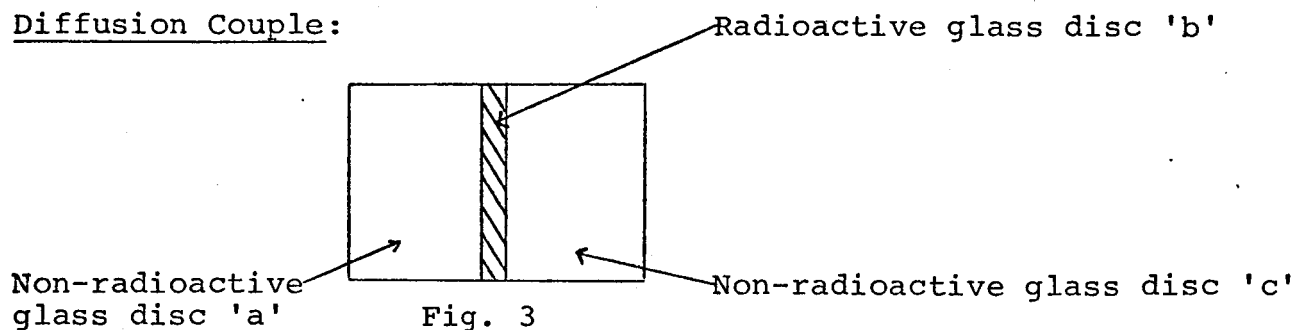


Fig. 3

The type of diffusion system used is shown in Fig. 3 and is the usual 'unidimensional sandwich couple' described by Crank. (§2.23., Mathematics of Diffusion, Oxford Press).

Experimental procedure

A glass of nominal composition 20% K_2O , 20% SrO , 60% SiO_2 (wt %) was melted in an electric furnace to obtain about 1000 g of seed-free homogeneous glass.

Cylindrical discs of 8.45 mm diameter with flat faces polished were prepared from this stock to correspond to the discs 'a', 'b' and 'c' of the diffusion couple. 'a' and 'c' were usually 3 mm thick whereas 'b' varied between 75 μ to 300 μ , the choice being dependent upon the objective of the particular experiment on hand.

Disc 'b' was made radioactive after exposing to a 10^{13} nv thermal neutron flux for 4-6 hours. The diffusion couple was enclosed inside a close-fitting steel box to maintain its geometry, and inserted into a furnace at the desired temperature, held for a specified time, removed and rapidly cooled to room temperature.

The specimen was machined on a jeweller's lathe to remove the original cylindrical surface and to expose the diffusion zone by removing most of the disc 'c'.

Progressive etching was then carried out with a 5% HF solution to dissolve layers perpendicular to the diffusion direction. The position of these layers was recorded with a dial indicator to an accuracy of 1.25μ .

γ activity in these solutions was counted using a 4" NaI (Tl) crystal in conjunction with a 256 channel analyzer. β activity was measured by employing a 2" Anthracene crystal and the 256 channel analyzer.

A flame photometric determination of the potassium content in these solutions to the accuracy of 1% provides a reliable means of determining the thickness of each layer.

Experiments so far carried out have enabled measurement of D for K and Sr over a range of temperatures. Where as a single experiment yields the values of D_K and D_{Sr} simultaneously by means of γ counting, it has not been possible to obtain D_{Si} by means of β counting from the same experiment due to the interfering β activity of K^{42} .

Therefore, small quantities of the same composition of

glass were melted which contained potassium as 99.97% K^{39} species (obtained from ORNL). This brought the activity of K down by a factor of about 200, enabling a more efficient separation of Si^{31} from the rest on the basis of shape of spectra and the half lives. Errors are still involved due to presence of Na^{24} impurity, though it has been possible to obtain values of D for Si within an order of magnitude.

SUMMARY OF THE RESULTS

Table V lists the diffusion coefficient values of K, Sr and Si over a range of temperatures. While none of the values have been analyzed for the associated errors (less than 10% for values $>10^{-9}$ cm^2/sec , less than 50% for values between 10^{-11} - 10^{-9} cm^2/sec), there seems to be conclusive evidence that $D_K \gg D_{Sr} > D_{Si}$ at a particular temperature. Experimental data from more of such experiments is yet to be processed and is hoped to be ready shortly in the form of a Master's thesis.

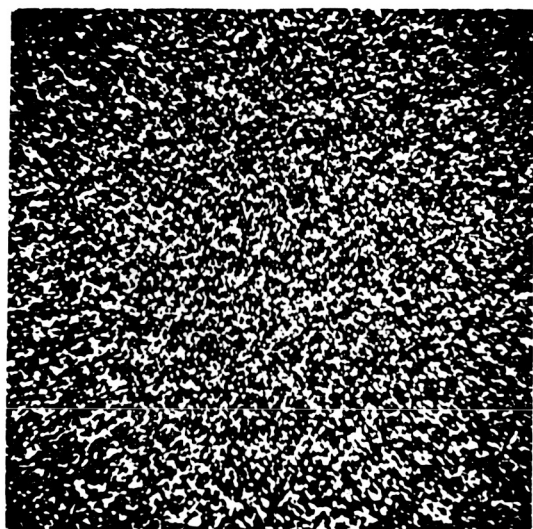
TABLE V

DIFFUSION COEFFICIENT (cms^2/sec) OF POTASSIUM, STRONTIUM
AND SILICON

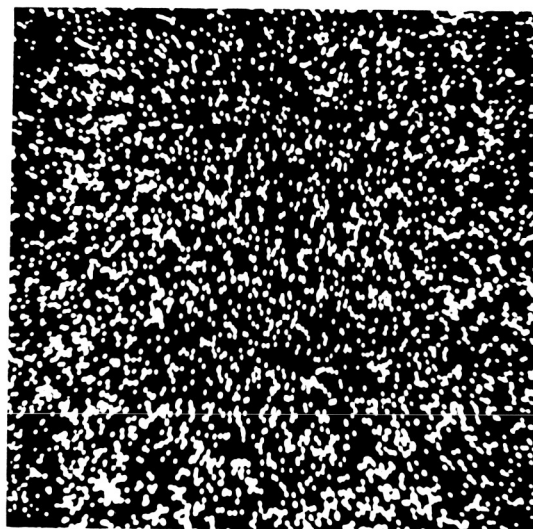
	D_K	D_{Sr}	D_{Si}
<u>Temperature</u>			
830°C	1.6×10^{-7}	6.3×10^{-10}	
765°C	8.3×10^{-8}	5×10^{-10}	
750°C	7.5×10^{-8}	- - - - -	$\sim 10^{-11}$
706°C	3.3×10^{-8}	1×10^{-10}	
660°C	3.8×10^{-9}	2.9×10^{-11}	
580°C	2.5×10^{-10}	4×10^{-12}	

PLATE 1:

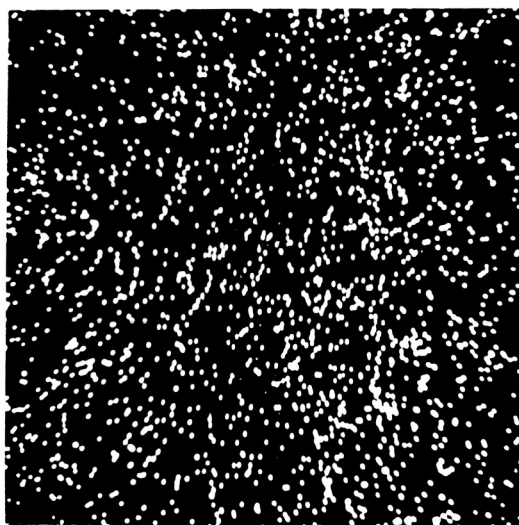
Compositional Variation of a Thailand Tektite
(X-ray distribution of elements over the same area of $80\mu \times 80\mu$)



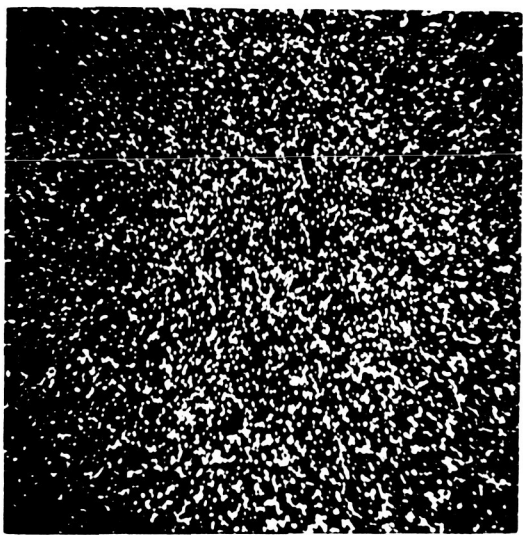
SILICON



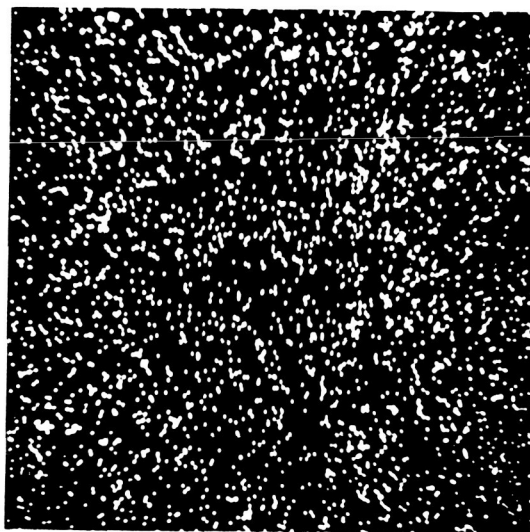
ALUMINUM



CALCIUM



POTASSIUM



IRON

FIG. 1a

SPEC. No.1
ALUMINUM

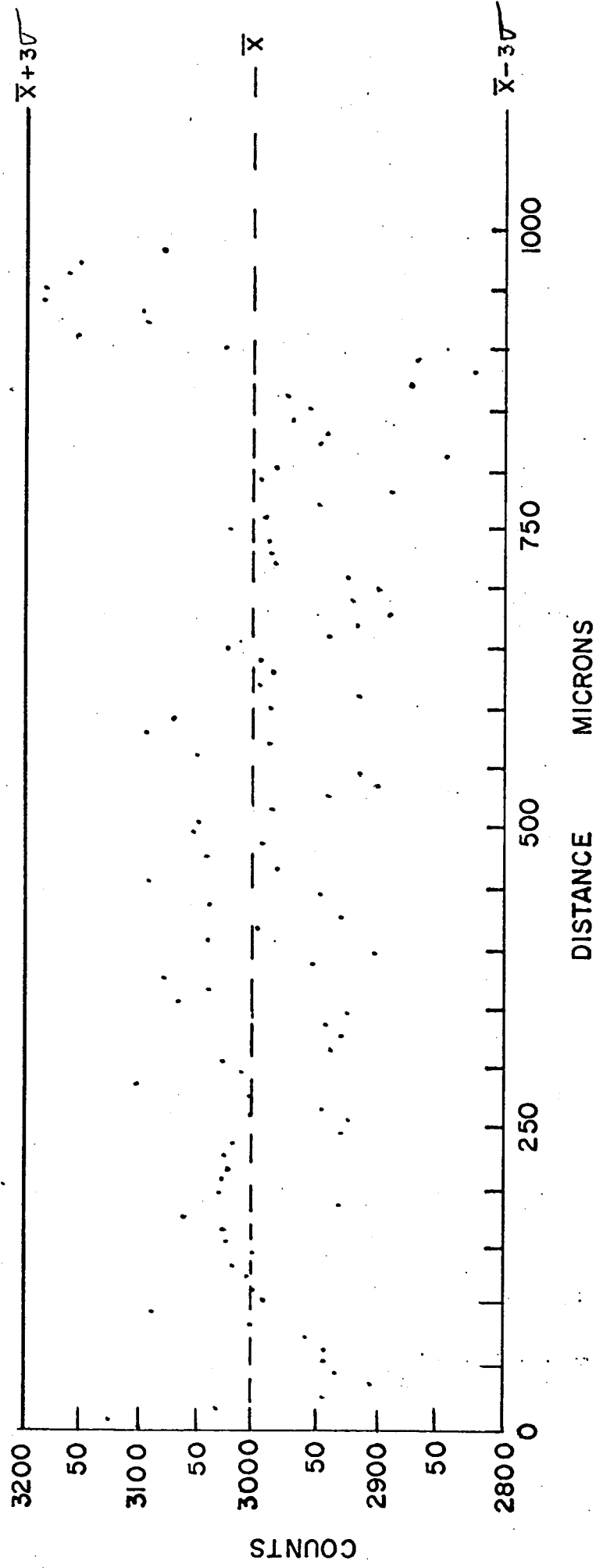


Fig. 1a Concentration Variation
With Position across 1 mm of:
Aluminum in Tektite

Fig. 1b Concentration Variation
With Position across 1 mm of:
Aluminum in Tektite

FIG: 1b

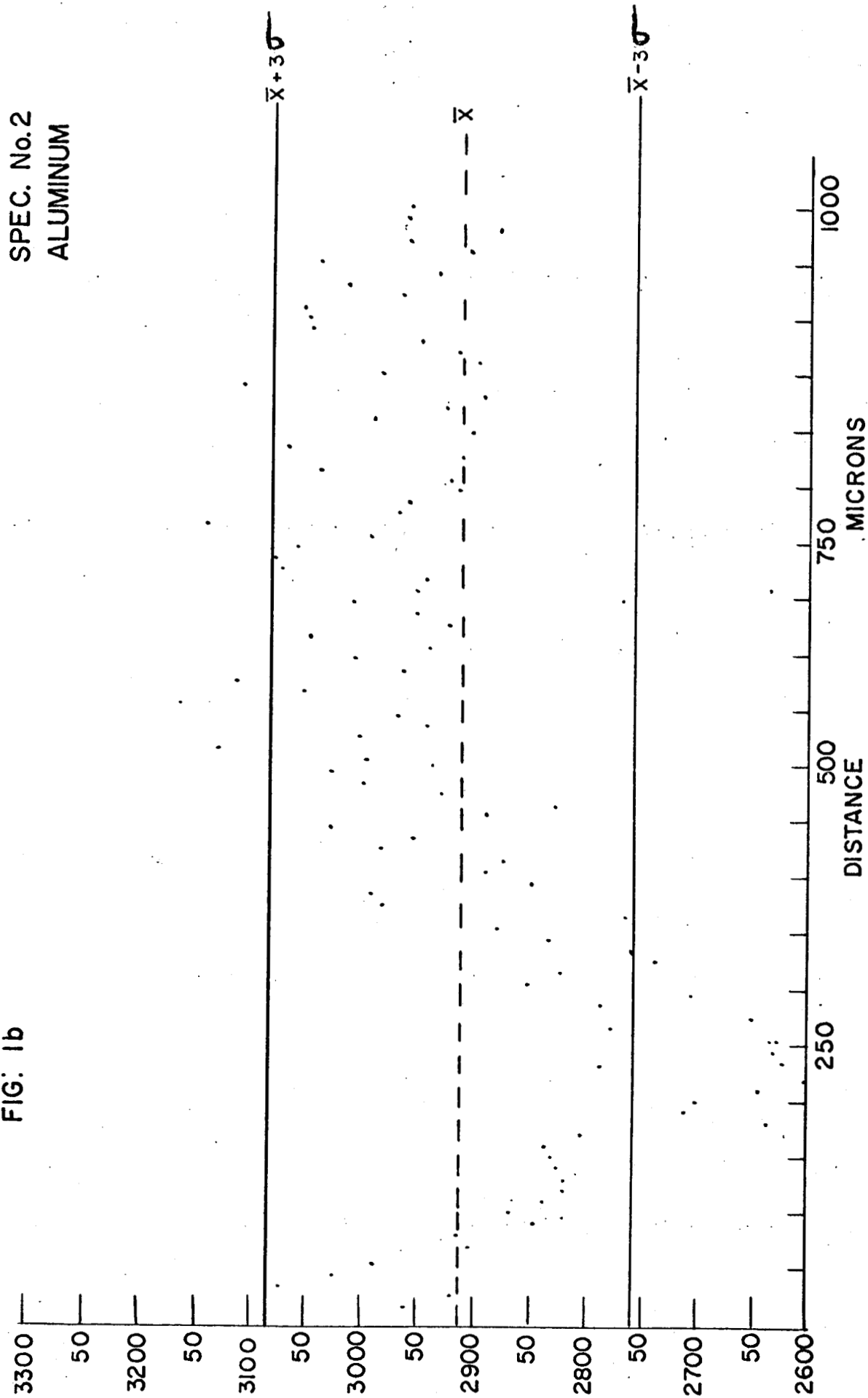


Fig. 1c Concentration Variation
With Position across 1 mm of:
Silicon in Tektite

FIG. 1c

SPEC. No. 1
SILICON

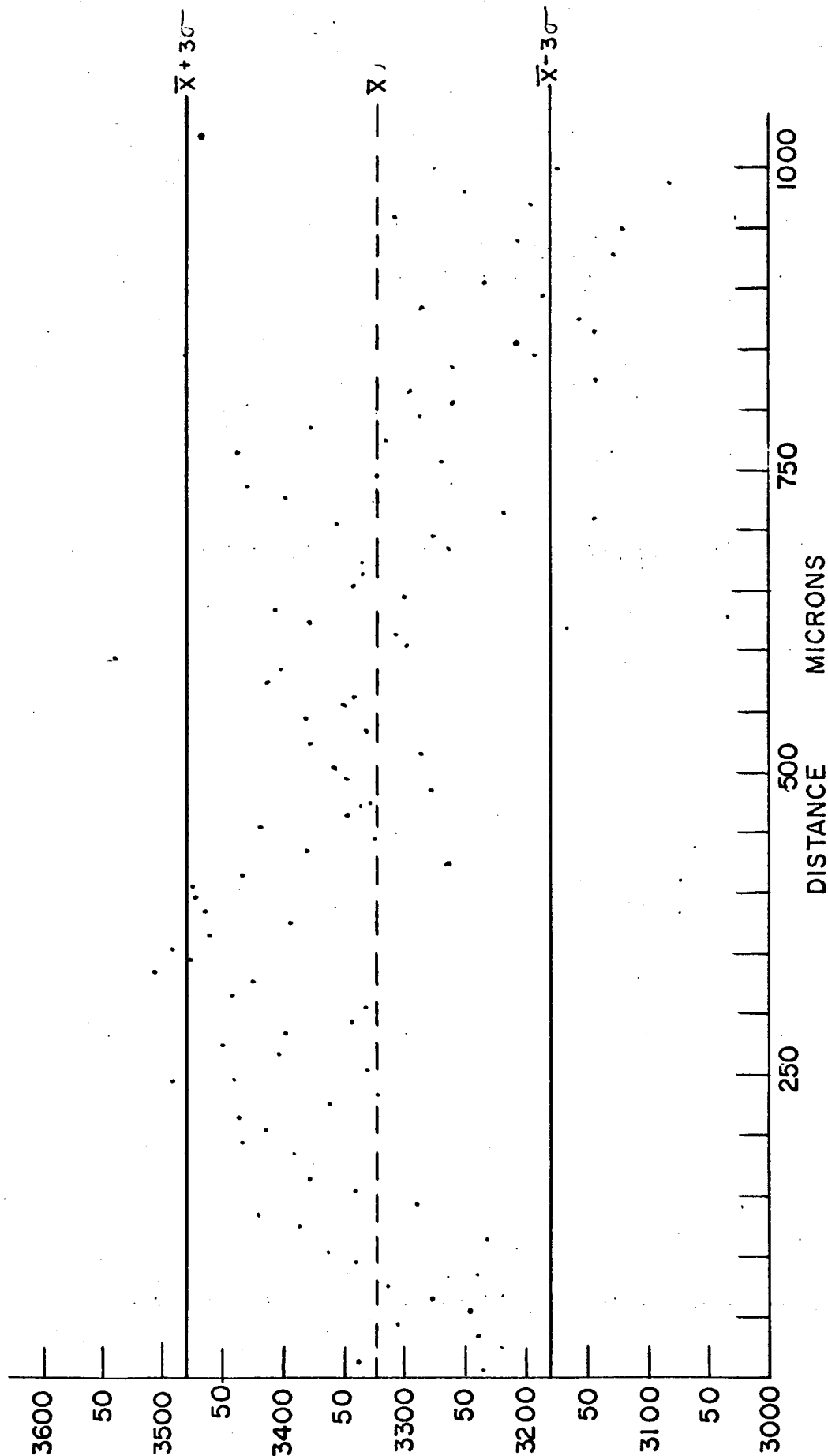


FIG. 1d

SPEC. No. 2
SILICON

$\bar{X} + 3\sigma$

Fig. 1d Concentration Variation
With Position across 1 mm of:
Silicon in Tektite

\bar{X}

$\bar{X} - 3\sigma$

COUNTS

DISTANCE MICRONS

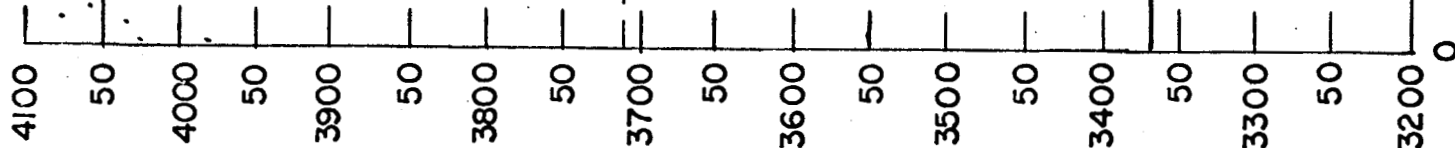


FIG. 1e

SPEC. No. L

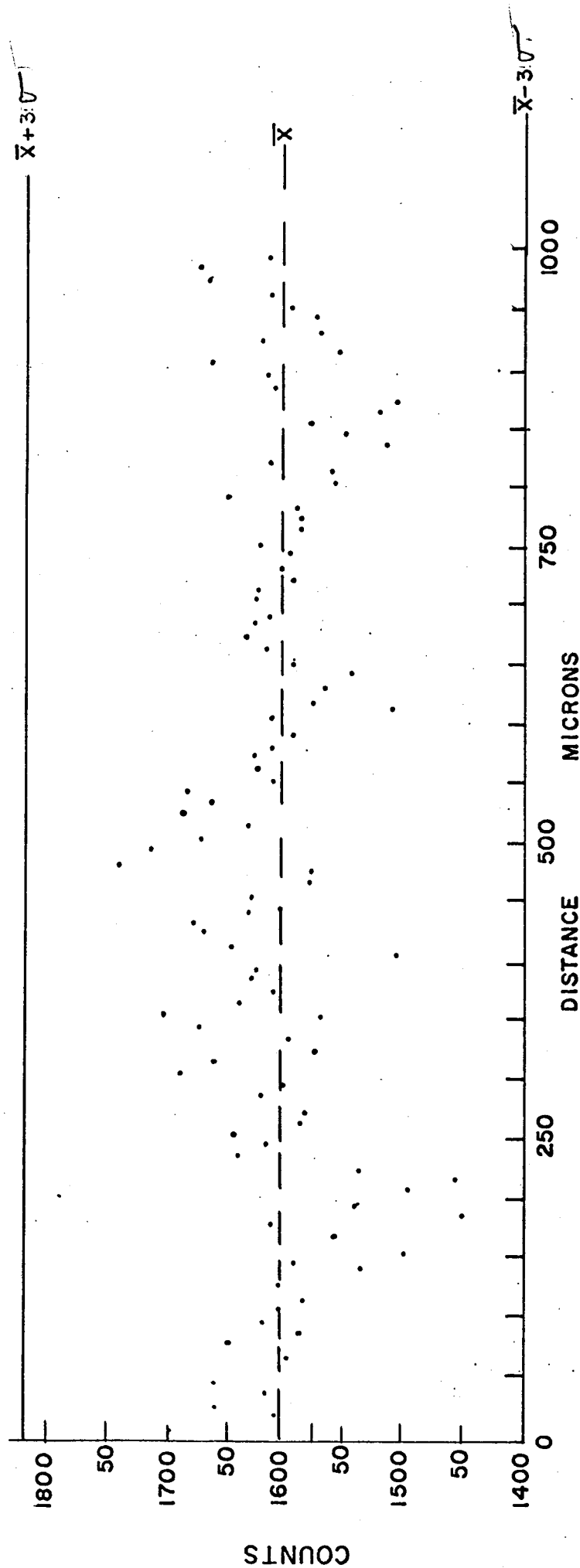


Fig. 1e Concentration Variation
With Position across 1 mm of:
Iron in Tektite

FIG. 1f

SPEC. No. 2
IRON

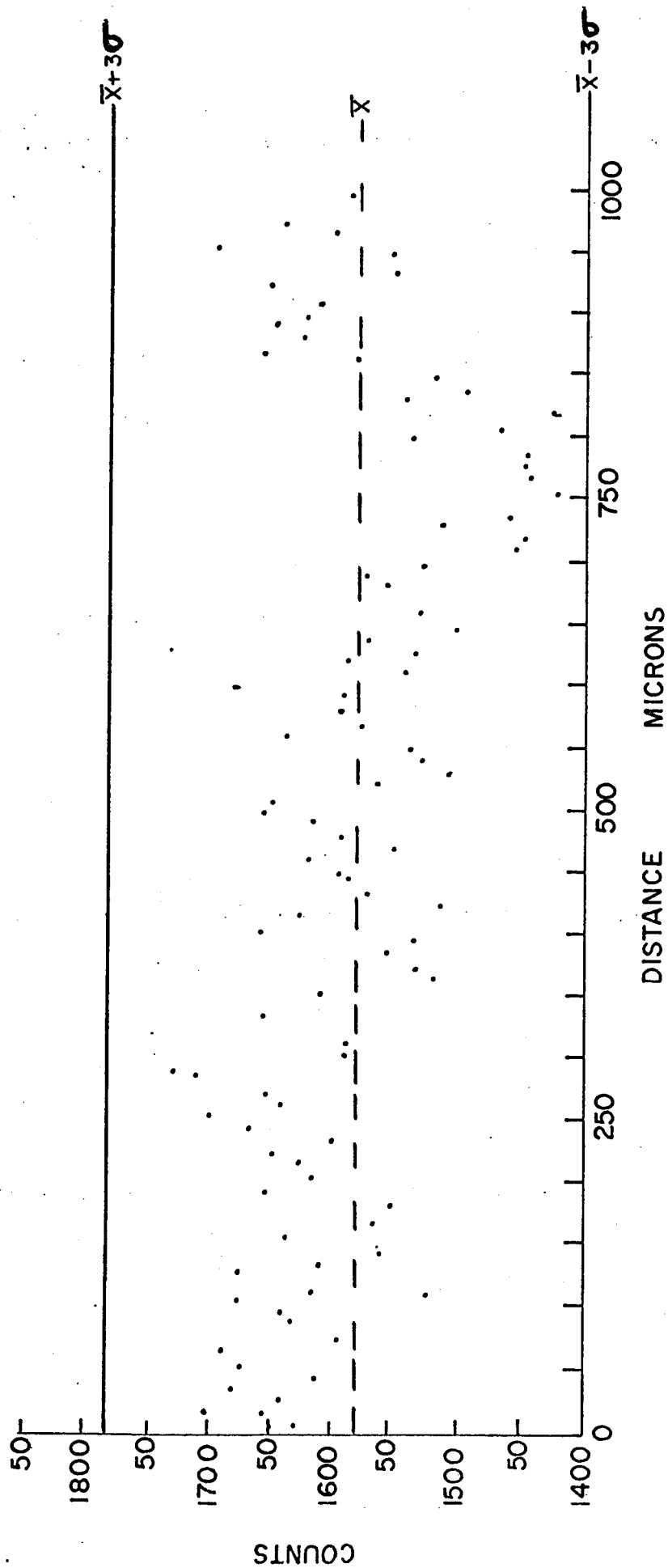


Fig. 1f Concentration Variation
With Position across 1 mm of:
Iron in Tektite

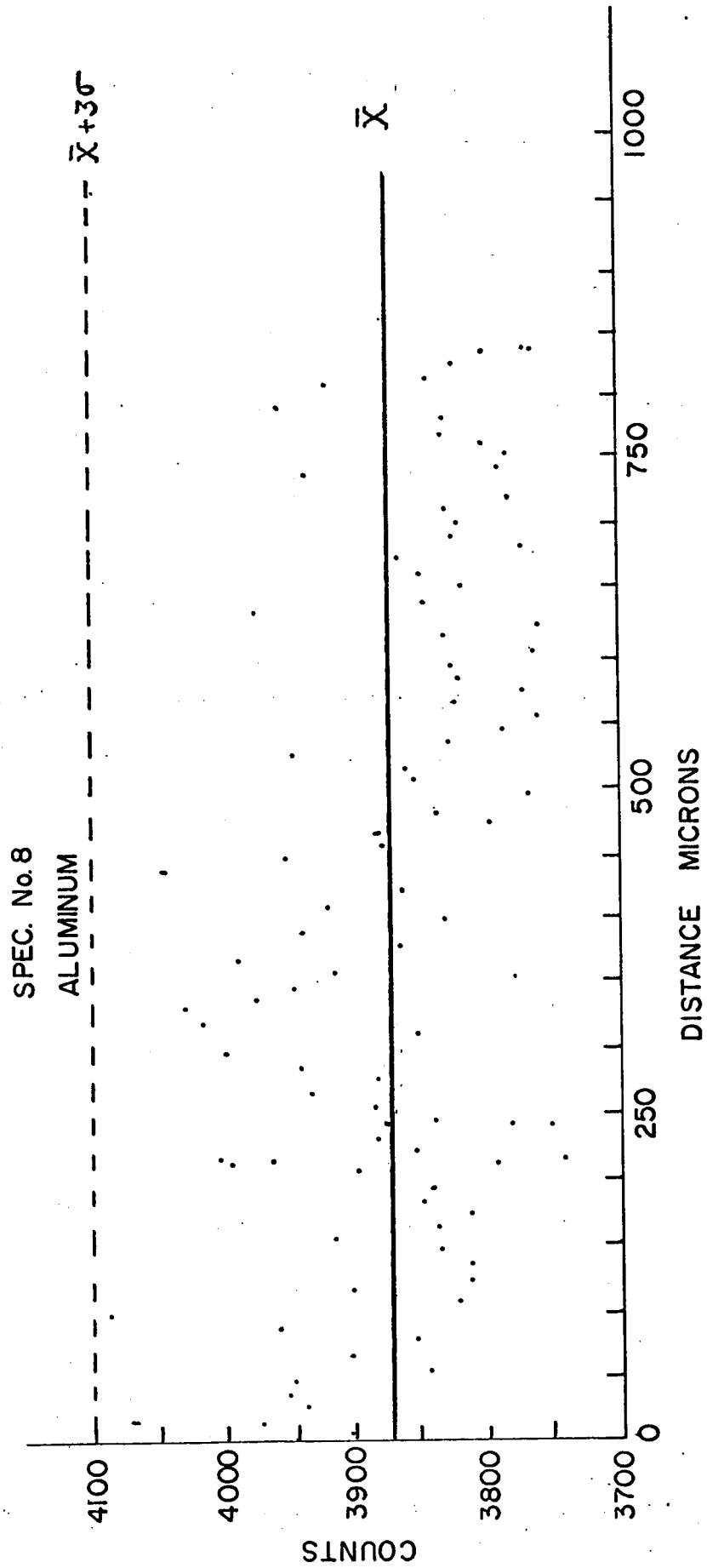


FIG. 1g: CONCENTRATION VARIATION WITH POSITION ACROSS IMM OF:
ALUMINUM IN SYNTHETIC TEKTITE.

FIG. 2a

SPEC. No. 1
ALUMINUM

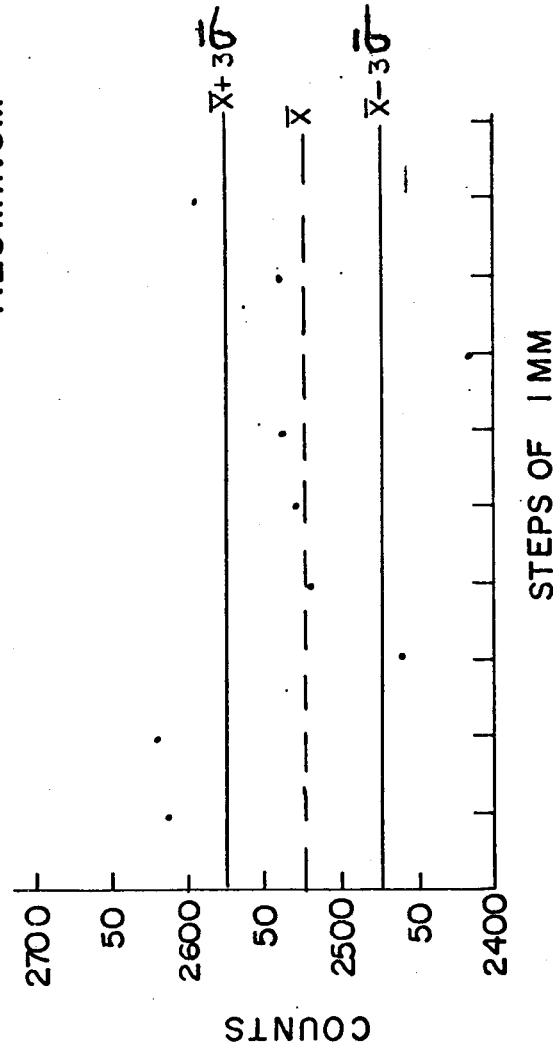


Fig. 2a Concentration Variation
With Position across 1 cm of:
Aluminum in Tektite

N.B.:- $\sigma \approx \sigma_5$

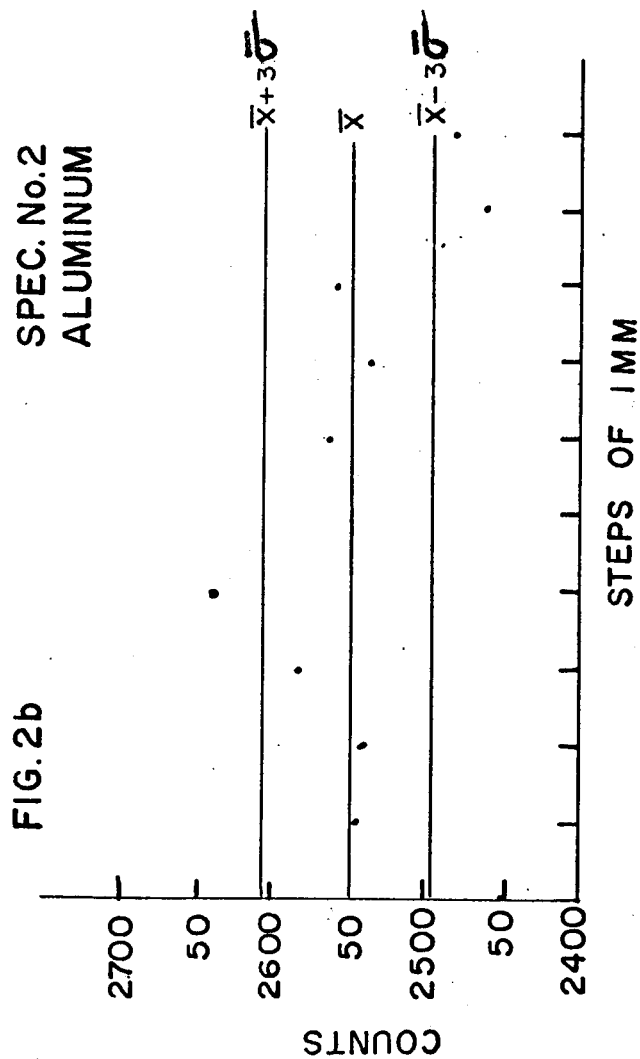


Fig. 2b Concentration Variation
With Position across 1 cm of:
Aluminum in Tektite

SPEC. No. 1
SILICON

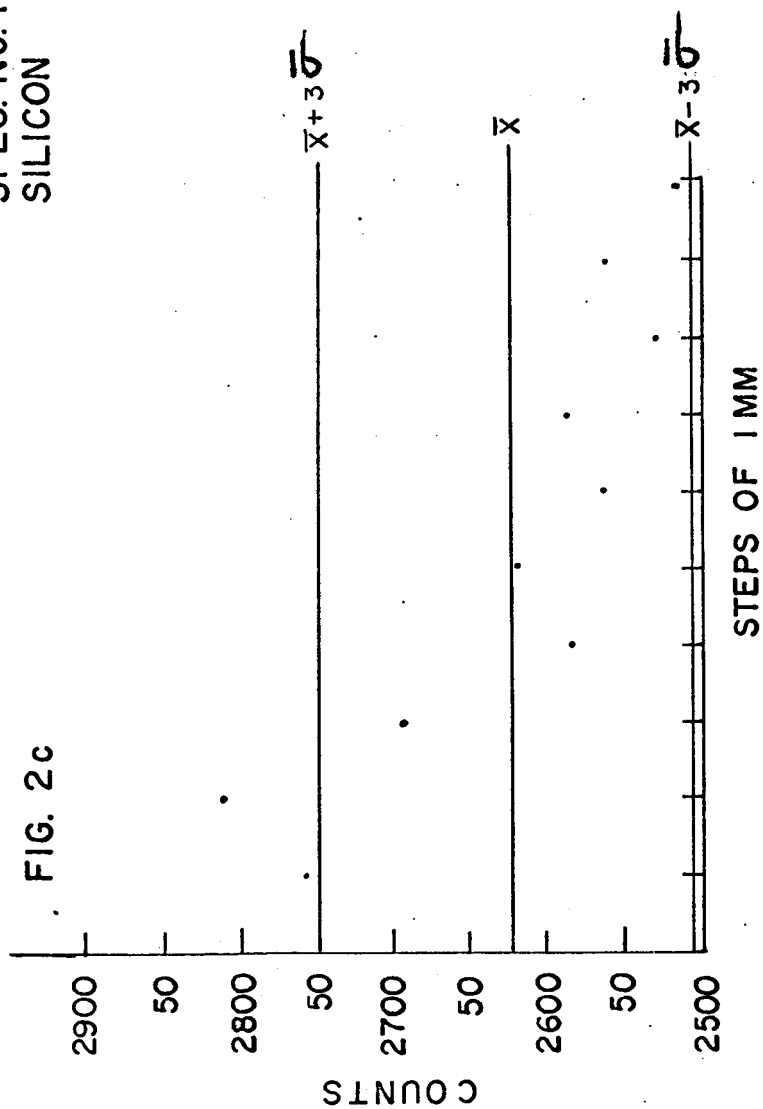


Fig. 2c Concentration Variation
With Position across 1 cm of:
Silicon in Tektite

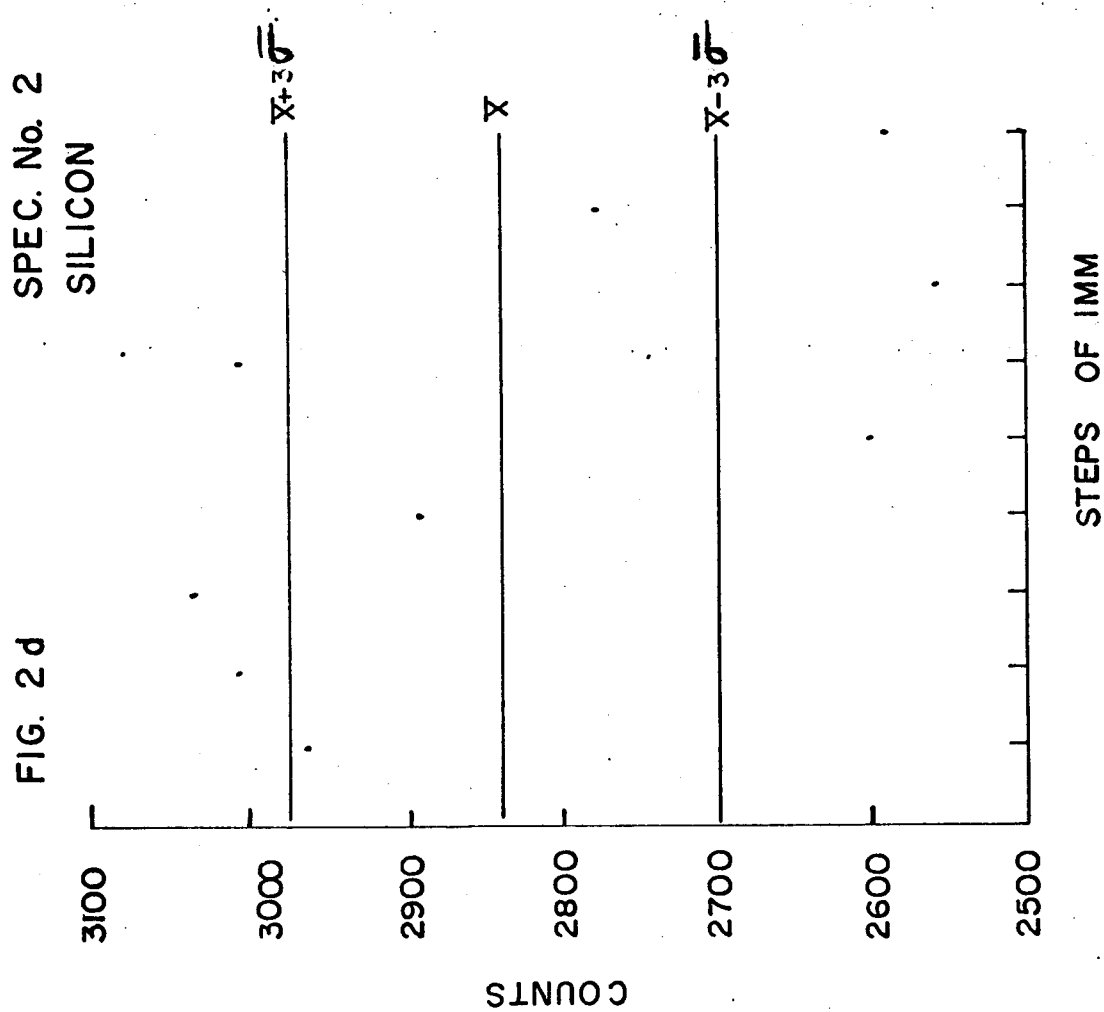


Fig. 2d Concentration Variation
With Position across 1 cm of:
Silicon in Tektite

FIG. 2e SPEC. No.1
IRON

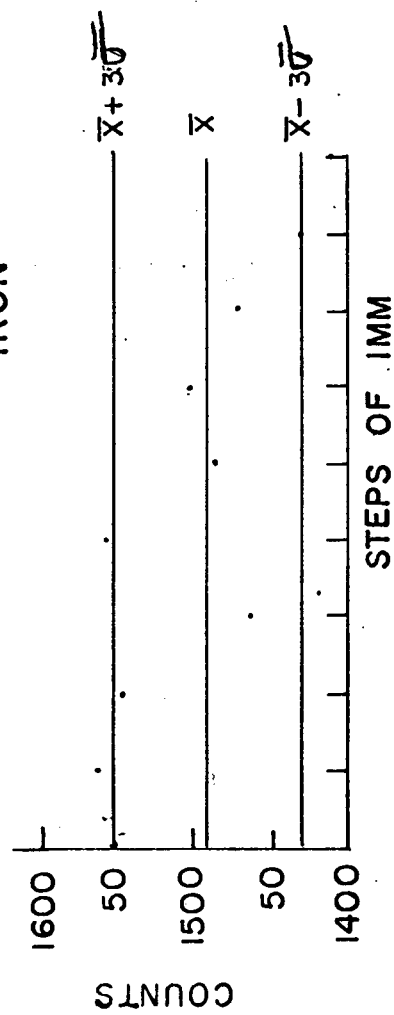


Fig. 2e Concentration Variation
With Position across 1 cm of:
Iron in Tektite